Journal of Structural Geology, Vol. 8, No. 7, pp. 781 to 798, 1986
Printed in Great Britain

0191-8141/86 $03.00 + 0.00
Pergamon Journals Ltd.

Dating of deformation phases using K–Ar and $^{40}Ar/^{39}Ar$ techniques: results from the Northern Apennines

ROY KLIGFIELD

Department of Geological Sciences, University of Colorado, Boulder, Colorado 80309, U.S.A.

JOHANNES HUNZIKER

Abteilung für Isotopen-Geologie, University of Bern, Bern CH 3012, Switzerland

R. D. DALLMEYER

Department of Geology, University of Georgia, Athens, Georgia 30602, U.S.A.

and

STEVEN SCHAMEL

Earth Science Research Institute, University of S. Carolina, Columbia, South Carolina 29208, U.S.A.

(*Received* 25 *February* 1985; *accepted in revised form* 6 *December* 1985)

Abstract—Paleozoic to Oligocene metasedimentary rocks present in the Alpi Apuane region of the Northern Apennines, Italy, have been sequentially deformed during a Tertiary progressive deformation. In an attempt to date the individual deformation episodes, over 50 conventional K–Ar and 11 $^{40}Ar/^{39}Ar$ incremental gas release analyses have been carried out on fine grained white micas separated from samples whose structural settings were well known. Mineralogy, X-ray diffractometry, and thin-section analyses indicate that the constituent muscovite and phengite formed under metamorphic conditions of 3–4 kbars and 300–400°C during all deformational phases. Pre-existing micas were variably crenulated during each subsequent deformational phase. Both K–Ar and $^{40}Ar/^{39}Ar$ analyses were carried out on 0.6–2 μm, 2–6 μm and 6–20 μm size separates of the phengitic white mica. Although the K–Ar apparent ages range from 11 to 27 Ma and are consistent with available stratigraphic constraints, the $^{40}Ar/^{39}Ar$ age spectra display variable internal discordancy. These isotopic data indicate that: (1) both the K–Ar and $^{40}Ar/^{39}Ar$ total-gas ages decrease as the degree of crenulation increases; (2) the K–Ar and $^{40}Ar/^{39}Ar$ total-gas ages decrease as grain size decreases; (3) for each sample, characteristics of the $^{40}Ar/^{39}Ar$ age spectra depend upon grain size, with fine sizes yielding discordant patterns which systematically increase in apparent age from low to high temperature and (4) phengitic micas associated with earliest structures yield generally older ages than micas associated with later structures.

The isotopic results are interpreted to indicate that the major deformation phase (D_1) occurred at approximately 27 Ma with subsequent pulses ending by *c.* 10 Ma. These results may be combined with finite strain data to suggest that the region was deformed at strain rates between 10^{-15} and 10^{-14} s^{-1}. A 27 Ma age indicates Mid-Oligocene initiation of plate tectonic activity in the Western Mediterranean and concomitant deformation in the Northern Apennines.

INTRODUCTION

AGE RELATIONSHIPS in polydeformed metamorphic terranes have been the subject of considerable investigation by structural geologists, petrologists and mineralogists. The chronologic relationships between nucleation, grain growth and strain events have traditionally been used to classify minerals as pre-, syn- or post-tectonic with respect to individual deformational phases (e.g. Spry 1969). However, a basic limitation of this method is that the mineral is only assigned an age relative to a structural 'event' and not relative to a framework of geologic time.

In greenschist facies metamorphic rocks, the presence of syntectonic micas (typically muscovite and/or phengite) provides an opportunity to obtain K–Ar mineral ages which may closely date individual deformational phases. In regions which have been repeatedly deformed and metamorphosed, the problems associated with diffusive loss or gain of radiogenic ^{40}Ar, combined with the difficulties involved in preparation of high-quality mineral concentrates serve to make this task difficult. Several recent studies have shown that analyses of carefully selected and prepared fine-grained samples do provide radiometric ages which may be useful in resolving chronologic relationships in low-grade, polydeformed terranes (Hunziker 1974, Odin *et al.* 1975, Ahrendt *et al.* 1977, 1978, Kroner & Clauer 1979, Dallmeyer 1979).

During structural mapping of deformed metasedimentary rocks in a portion of the Northern Apennines, it became apparent that the significance of previous K–Ar age determinations (Giglia & Radicati de Brozolo 1970) was uncertain. Detailed structural fieldwork during the last decade has provided an exceptionally clear picture of this region which underwent a series of deformational

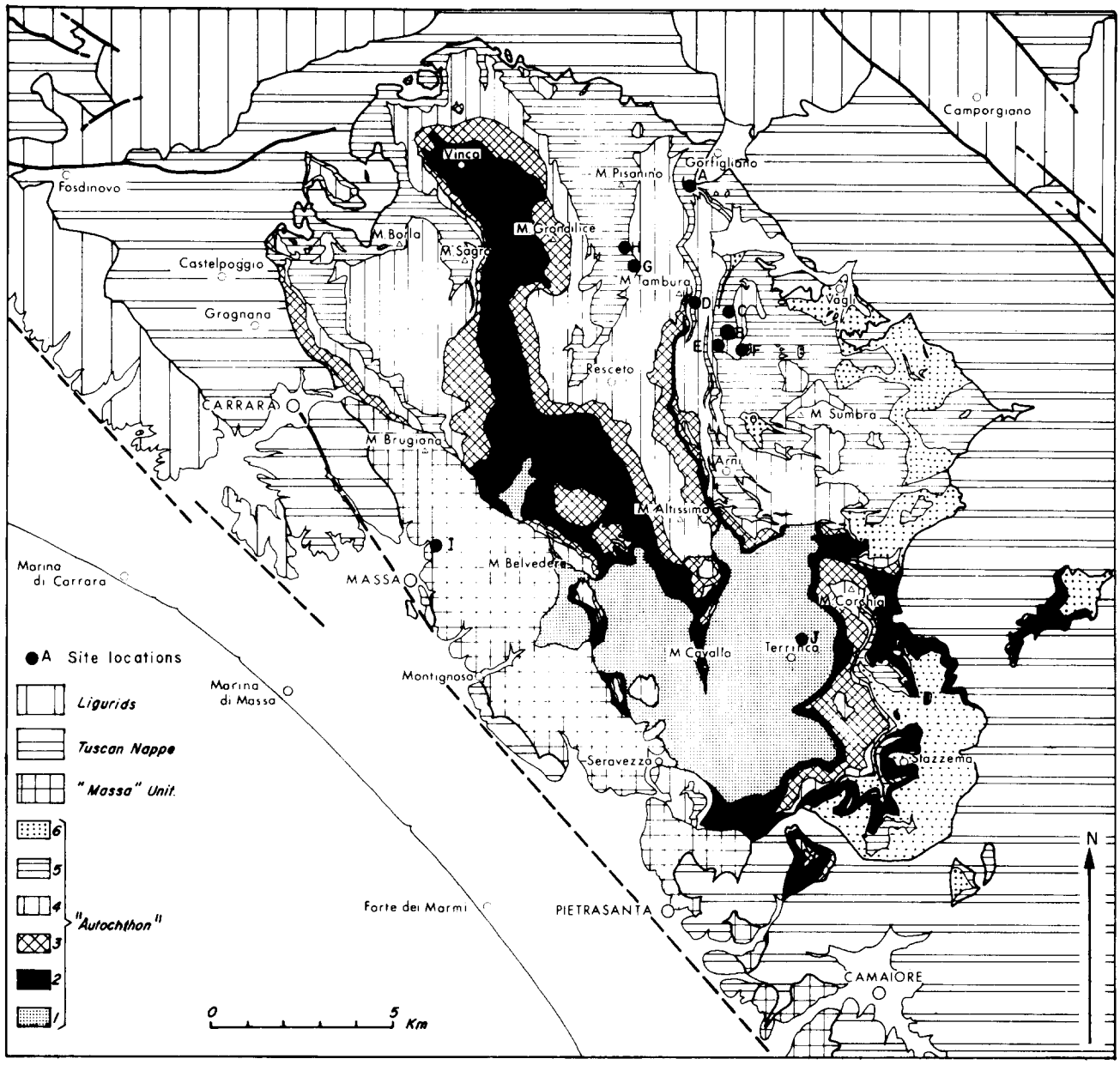

Fig. 1. Geologic map of the Alpi Apuane region of Italy and site locations of dated material. Letters beside site localities refer to samples listed in Tables 1, 2 and 4. Key to symbols: 1, Paleozoic basement complex; 2, Porphyroid schists; 3, dolomite (Norian); 4, marble (Liassic); 5, cherty limestone, radiolarian chert and cherty schists, calcschists, sericite shales and slates (Cretaceous–Eocene); 6, turbiditic flysch (Oligocene). Normal faults are shown by dashed and solid heavy lines. Samples of Giglia & Radicati di Brozolo (1970) come from the Arni locality.

pulses, all belonging to a single overall progressive phase of Tertiary deformation (Carmignani *et al.* 1978). In an effort to provide more complete chronologic constraints and to date the individual pulses within the overall progressive deformation, a detailed K–Ar and $^{40}Ar/^{39}Ar$ geochronological study has been carried out. Results of this study are reported here and discussed in terms of: (1) age results for syntectonically recrystallized muscovites and phengites; (2) the effects of redeformation (crenulation) on isotopic systems and (3) the significance of age variations related to variations in grain size. The isotopic data yield chronologic brackets for the Tertiary deformational and metamorphic events recorded in this area. These provide regional constraints for various tectonic models proposed for the evolution of the Northern Apennine mountains in the overall context of the Western Mediterranean region.

GEOLOGICAL SETTING

Tectonic framework

Metasedimentary rocks of the Alpi Apuane region of Italy are exposed in a large tectonic window through a series of overlying, generally non-metamorphosed allochthonous sequences which constitute most of the Northern Apennine terrane (Fig. 1). These nappes were transported northeastward onto the Northern Apennine continental margin during Oligocene collision with the

Corsican microcontinent (Kligfield 1979). Descriptions of the lithologic characteristics, structural history, metamorphic record, and tectonic evolution of the Northern Apennines may be found in an extensive literature (Dallan-Nardi & Nardi 1974, Elter *et al.* 1975, Gianninni & Lazzarotto 1975, Carmignani *et al.* 1978) and are not reviewed here.

Stratigraphy

What appears to be the structurally lowest portion of the metamorphic succession is represented by a series of interfoliated phyllite, schist, albite–gneiss and quartzite. A Paleozoic age for this sequence is clearly suggested by both the presence of Silurian fossils (Vai 1970, Bagnoli & Tongiorgi 1979) and local structural documentation of pre-Triassic deformation (Barberi & Giglia 1965). A lithologically similar terrane, exposed within the Mt. Pisani tectonic window 30 km south of the Alpi Apuane, contains a diverse Paleozoic fossil assemblage (Rau & Tongiorigi 1974) and records Rb–Sr radiometric evidence of a Hercynian (*c.* 285 Ma) tectonothermal event (Borsi *et al.* 1967).

In the Alpi Apuane region, clastic and volcanoclastic metasediments of ?Late Permian and Triassic age, the Verrucano Series, rest unconformably on the Paleozoic basement complex. Conformably overlying this is a thick succession of dolomitic marble and limestone marble of middle Triassic through Liassic age. A cherty limestone immediately overlying the marble marks a transition to more siliceous, deeper water sedimentation indicated by red, cherty schist containing radiolaria of Dogger–Malm age and sericitic phyllite and calcschist of Cretaceous to Eocene age. The youngest stratigraphic unit is the *pseudomacigno*, an Oligocene age distal turbidite (Dallan-Nardi & Nardi 1974, Carmignani *et al.* 1978) (Fig. 2). The pseudomacigno is the youngest unit affected by the Tertiary tectonothermal activity recorded in the Northern Apennines, and its stratigraphic age provides an important reference for comparison with K–Ar and $^{40}Ar/^{39}Ar$ mineral dates recorded in the metamorphic terrane. Dallan-Nardi (1977) correlated microfossils obtained from uppermost portions of the pseudomacigno with planktonic foraminiferal zones P18–20 of Blow (1969). Recent attempts at radiometric calibration of the Palaeogene time scale (Curry & Odin 1982) suggest these zones span a time of 34–27 Ma.

The Alpi Apuane region (Fig. 1) is cut by grabens containing undeformed sedimentary fill of Messinian age (Federici 1973). Lignite bearing, lacustrian marls present in the grabens are identical to a similar sequence of sediments further south near Grosetto (Lorenz 1968), which have been dated on the basis of their faunal assemblages at 8 Ma (Hurzeler & Engesser 1976). Their tectonic setting (Elter *et al.* 1975) is identical to that of the Alpi Apuane region. If the 8 Ma date recently suggested for the Tortonian–Messinian stage boundary by Tisserant & Odin (1979) is used, then penetrative tectonothermal activity must have ceased in the Alpi Apuane region prior to *c.* 8–7 Ma.

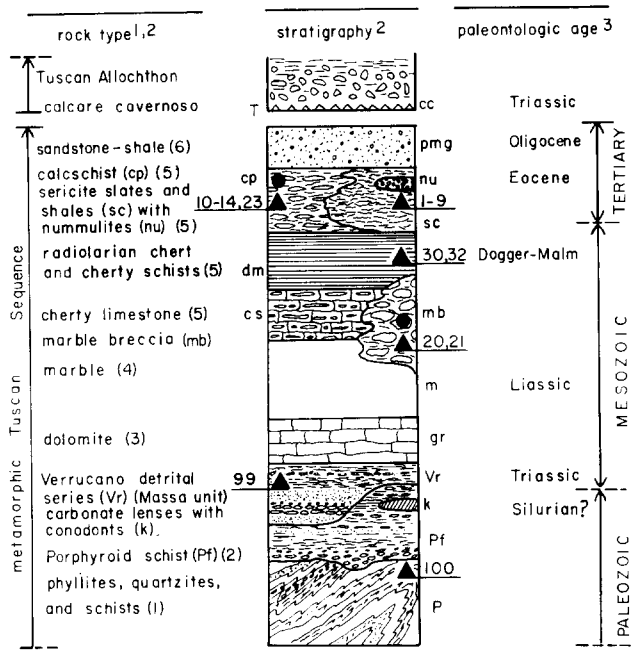

Fig. 2. Generalized stratigraphy of the metamorphic sequences in the Alpi Apuane region. Numbered black triangles show stratigraphic position and sample numbers of dated specimens. Sampling localities of Giglia & Radicati di Brozolo (1970) shown by unnumbered circles. Site locations and stratigraphy are indicated in Fig. 1. Letters are as follows: cc, calcare cavernoso; pmg, pseudomacigno turbiditic flysch; cp, cipollino calcschist; sc, sericite shale and slate; nu, nummulitic microbreccia; dm, radiolarian chert and cherty schist; cs, cherty limestone; mb, marble breccias; m, marble, gr, "grezzoni" dolomite; Vr, "Verrucano" detrital sequences in the Massa unit; Pf, porphyroids and porphyroid schists; P, phyllites, schists and quartzites of the basement complex. Paleontological ages taken from Dallan-Nardi & Nardi (1974), Carmignani & Giglia (1975) and Dallan-Nardi (1977).

Metamorphism

Metamorphic rocks of the Alpi Apuane region record mineral assemblages typical of the chlorite and biotite zones of the greenschist facies (Giglia 1967). Typical metamorphic parageneses in pelitic rocks include quartz, phengitic white mica, chlorite, calcite, albite, epidote, and locally biotite and/or chloritoid. Material analyzed isotopically in this investigation has been examined with X-ray diffraction methods to further clarify the metamorphic parameters. These results are discussed in a subsequent section.

Deformation phases

The structural evolution of the Alpi Apuane region has been interpreted in terms of the development of a large scale, overthrust type, simple-shear zone developed along the Northern Apennines continental margin during the Tertiary. As part of the progressive simple-shear deformation which occurred, several distinct phases of post-Paleozoic deformation have been described; together, these deformation pulses contributed to the build up of the strains observed (Carmignani & Giglia 1975, 1977, 1979, Carmignani *et al.* 1978, Kligfield *et al.* 1981, Kligfield 1979, 1980).

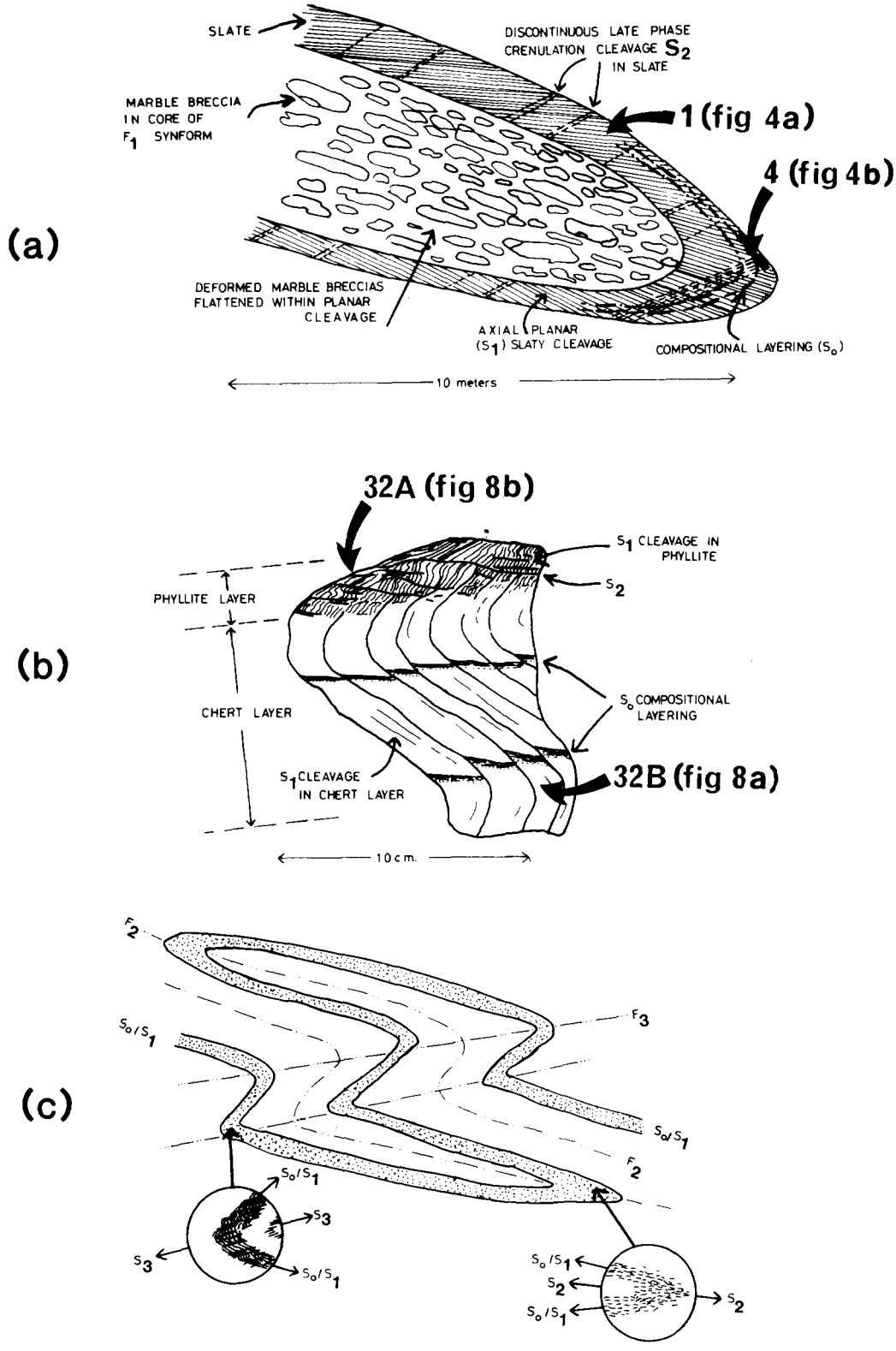

Fig. 3. Structural relationships in Alpi Apuane metasediments. D, deformation phase; F, folding phase; S, schistosity. (a) Fabric relationships in F_1 synform in slate cut by discontinuous D_2 crenulation cleavage (samples 1–4). (b) Typical D_1/D_2 relations in cherty schists (samples 30–32 and 20). (c) D_3 late stage refolding of earlier D_1 and D_2 structures in calcschists (samples 10, 11, 23). The orientations of white K micas and chlorites are shown schematically in the cores of the folds.

The earliest Tertiary deformation phase (D_1) produced mega- and mesoscopic isoclinal folds and resulted in development of a regionally penetrative foliation (S_1). Two subsequent deformational phases, although locally significant on the mesoscopic scale, are not regionally penetrative. A D_2 event involved two pulses termed D_{2A} and D_{2B} by Kligfield (1978). These are diachronously related in space and time and were previously termed D_2 and D_3 by Carmignani *et al.* (1978) and Carmignani & Giglia (1979). D_2 phase deformation is locally manifested by the development of crenulation cleavage, differentiated crenulation cleavage (Borradaile *et al.* 1982), kink bands, and conjugate folds (Fig. 3). Similar structures were produced during a later

deformational phase termed D_3 by Kligfield (1978). The D_1, D_2 and D_3 deformational phases appear to have been followed locally by post-tectonic growth of randomly oriented, phengitic white mica.

Field observations, thin-sections, and results of scanning electron microscopy suggest that distinct phases of white mica growth at least locally accompanied each of the three deformational phases. Oriented white micas define an S_1 foliation which clearly transects primary compositional layering within hinge zones of most F_1 isoclinal folds (Fig. 3). The D_{2A} and D_3 phases were locally sufficiently penetrative to produce growth of white mica along S_2 and S_3 foliations (Fig. 3). None of the samples analyzed in this investigation contain D_{2B} fabrics whose geographic distribution is limited.

PREVIOUS GEOCHRONOLOGY

Previous geochronological studies have been carried out within Paleozoic basement rocks of the Mt. Pisani tectonic window, to the south of the present field area. A Rb–Sr whole-rock isochron age of 285 ± 12 Ma (initial Sr ratio of 0.712, recalculated from Borsi *et al.* 1967) was obtained on a series of Paleozoic phyllites. This age was interpreted to record a Hercynian phase of orogenesis, and display no effects of subsequent Tertiary deformation and metamorphism.

K–Ar ages from the Triassic to Tertiary cover sequence of the Alpi Apuane region were reported by Giglia & Radicati di Brozolo (1970). They presented K–Ar ages on >70 μm size fraction separates of white mica ranging from 17.0 to 10.8 Ma. Their sample localities were revisited during the present investigation. All sites sampled by Giglia & Radicati di Brozolo (Fig. 2) show the effects of extensive deformation of S_1 white micas as a result of local D_2 and D_3 phase transposition.

SAMPLING

Field sampling was coordinated to obtain samples which contain white micas associated with the different structural phases. The presence of white micas younger than the D_1 phase appears to be controlled structurally on a very local scale by the non-penetrative development of a differentiated crenulation cleavage in slates and a spaced, disjunctive foliation (of presumably pressure solution origin) in other lithologies. It was anticipated that samples collected at different locations within an individual exposure had the potential to yield white micas related to different structural generations. These could be separated for isotopic analysis either as a result of inherent differences in grain size and/or the local nature of the fabric development.

Samples were collected from sites distributed throughout the Jurassic to Oligocene age cover sediments of the Alpi Apuane region (Figs. 1 and 2, Table 4). The samples may be divided into slates, cherty schists and calc-schists (Fig. 2, Tables 1, 2). A set of whole rock samples was collected in the Paleozoic basement (100 series) and the Triassic Verrucano detrital rocks (99 series) in order to evaluate the suitability of whole rock samples. The results from this suite of samples are reported in Appendix 1.

ANALYTICAL TECHNIQUES

Sample preparation

K–Ar and $^{40}Ar/^{39}Ar$ isotopic ages were determined for 0.6–2, 2–6 or 6–20 μm size fractions prepared by settling methods from powdered specimens (see Weber 1972 for sample preparation techniques). The range within each size fraction has been checked by electron microscopy and has a Gaussian distribution with 2σ values between the ranges indicated. Various size fractions were treated with 5% acetic acid to remove carbonate. X-ray diffraction analyses of the powdered samples demonstrate that the size separates consist largely of phengite with small and variable amounts of chlorite.

X-ray diffraction studies

Illite crystallinity has been determined for most of the analyzed samples using the methods outlined by Kübler (1967). In addition, white mica compositions were estimated using the b_o diffraction spacing following the methods of Guidotti & Sassi (1976) using the revised calibration curves of Frey (1978).

ISOTOPIC ANALYSES

K–Ar *analyses*

A complete description of the analytical procedures followed during K–Ar age determinations may be found in Hunziker (1974). Argon was measured on a Varian GD 150 mass spectrometer using a 99.99% ^{38}Ar spike (Clausis, Zurich). The spike has been calibrated against both a U.S. Geologic Survey muscovite standard (P207) and a Bern muscovite standard (4M) using values of 28.15 and 6.31×10^{-6} cm^3 ^{40}Ar STP, respectively. Potassium was determined on a Beckman flame photometer. Apparent ages were calculated using the isotopic abundance ratios and decay constants listed by Steiger & Jäger (1977).

$^{40}Ar/^{39}Ar$ *incremental-release analyses*

The principles of $^{40}Ar/^{39}Ar$ incremental-release dating have been described by Dalrymple & Lanphere (1971), Dallmeyer (1979), and Dalrymple *et al.* (1981). The techniques used during analysis of the Alpi Apuane samples generally followed those described in detail by Dallmeyer & Rivers (1983). Variations in the flux of neutrons along the length of the irradiation assembly

Table 1. Sampling and measurement scheme for the Alpi Apuane cover rocks

Rock type	Structure	Site No.*	Sample No.*	Grain size†	K–Ar‡	$^{40}Ar/^{39}Ar$‡
Slate	Variably crenulated S_1 micas	A	1	0.6–2	x	x
Slate	Variably crenulated S_1 micas	A	1	2–6		x
Slate	Variably crenulated S_1 micas	A	1	6–20		x
Slate	Variably crenulated S_1 micas	A	2	0.6–2	x	
Slate	Variably crenulated S_1 micas	A	3	0.6–2	x	
Slate	Variably crenulated S_1 micas	A	4	0.6–2	x	
Slate	D_3 micas	C	23	0.6–2	x	x
Slate	D_3 micas	C	23	2–6	x	x
Slate	D_3 micas	C	23	6–20	x	x
Slate	Crenulated S_1 micas	E	20	0.6–2	x	
Slate	Crenulated S_1 micas	E	20	2–6		x
Slate	Variably crenulated S_1 micas	B	5	0.6–2	x	
Slate	Variably crenulated S_1 micas	B	6	0.6–2	x	
Slate	Variably crenulated S_1 micas	B	7	0.6–2	x	
Slate	Variably crenulated S_1 micas	B	8	0.6–2	x	
Slate	Variably crenulated S_1 micas	B	9	0.6–2	x	
Cherty schist	Uncrenulated S_1 micas with younger overgrowths	E	20B	0.6–2	x	
		E	20B	2–6		x
Cherty schist	Uncrenulated S_1 mica	G	32B	0.6–2	x	
	D_{2A} micas	G	32A	2–20	x	x
Calc-schists	D_{2A} and D_3 crenulations of S_1 micas	C	10	0.6–2	x	
Calc-schists	D_{2A} and D_3 crenulations of S_1 micas	C	10	2–20	x	
Calc-schists	D_{2A} and D_3 crenulations of S_1 micas	C	11	0.6–2	x	
Calc-schists	D_{2A} and D_3 crenulations of S_1 micas	D	14	0.6–2	x	
Calc-schists	D_{2A} and D_3 crenulations of S_1 micas	D	13	0.6–2	x	
Calc-schists	D_{2A} and D_3 crenulations of S_1 micas	D	13	2–6	x	x
Calc-schists	D_{2A} and D_3 crenulations of S_1 micas	D	13	6–20	x	

* Site and sample localities given in Figs. 1 and 2 and in Table 5.
† Grain size in μm.
‡ x indicates measurement made.

were monitored with several mineral standards, including MMhb-1 (Alexander *et al.* 1978).

Measured isotopic ratios were corrected for the effects of mass discrimination and the interfering isotopes produced during irradiation using the factors reported by Dalrymple *et al.* (1981) for the reactor used in the present study. Apparent $^{40}Ar/^{39}Ar$ ages were calculated from the corrected isotopic ratios using the decay constants and isotopic abundance ratios listed by Steiger & Jäger (1977). Total uncertainties in each apparent age are quoted at 2σ and have been calculated following the methods outlined by Dalrymple & Lanphere (1971).

X-RAY DIFFRACTION RESULTS

All size fractions of the phengitic white mica separates contain only $2M_1$ polytypes. The illite crystallinity values of the samples vary between 2.4 and 3.4 (Table 2). These values are within the range commonly associated with a greenschist-facies regional metamorphism (Frey 1969), and are consistent with the 275–375°C temperatures of metamorphism suggested by the partitioning of Mg between co-existing calcite and dolomite in Alpi Apuane marbles (Crisci *et al.* 1975) and the thermoluminescence curves reported for marbles of the Alpi Apuane region by D'Albissin (1963).

Examination of the b_o spacing of constituent white micas (Guidotti & Sassi 1976) within the various size samples analyzed suggests that both phengite ($d_{060} >$ 1.502 Å) and muscovite ($d_{060} >$ 1.502 Å) components are present. This is significant because Velde (1967) has experimentally shown that at *c.* 350°C both phengite and muscovite coexist under confining pressures between *c.* 3 and 4 kilobars. Together, the regional mineral assemblages, the character of illite crystallinity, and the white mica compositions suggest that temperatures of *c.* 350–400°C and confining pressures of *c.* 3–4 kilobars were probably maintained during the Tertiary tectonothermal activity recorded in the Alpi Apuane region.

ISOTOPIC RESULTS

Both conventional K–Ar and $^{40}Ar/^{39}Ar$ results have been obtained in the Triassic to Oligocene age cover rocks. A summary of rock type, size fraction of mineral

Table 2. Isotopic data for conventional K–Ar measurements, illite crystallinity and b_0 values of micas

Sample*	Rock type†	Mineral‡	Size§ fraction	^{40}Ar rad $cm^3\,10^{-6}\,g^{-1}$ STP	% rad	% K	$^{40}Ar/^{36}Ar$	$^{40}K/^{36}Ar$	Age Ma‖ + Ma	d_{060} of K mica	Illite crystallinity
0	—	Qt 2	—	0.40	20.0	—	380.0	0	—		
1	S	Ph-Chl	<0.6	5.69	71.4	6.40	1039.7	559.7	22.7 ± 0.9		
1	S	Ph-Chl	0.6–2	5.66	79.8	5.85	1466.0	809.2	24.6 ± 0.9	1.5075	3.4
1	S	Ph-Chl	2–6	4.72	69.8	4.85	985.6	474.3	24.8 ± 0.9		
2	S	Ph-Chl	<2	3.22	70.8	5.76	1011.0	857.1	14.2 ± 0.6	1.5075	3.3
3	S	Ph-Chl	<2	4.86	84.2	4.56	1942.0	1034.0	27.0 ± 1.0	1.5009	3.2
4	S	Ph-Chl	<2	5.21	60.4	6.04	1139.0	654.9	21.9 ± 0.9	1.5044	3.0
5	S	Mu-Chl	<2	2.16	53.1	2.59	630.3	268.1	21.2 ± 1.2	1.4997	3.2
6	S	Ph-Chl	<2	2.52	66.1	3.62	871.7	553.7	17.7 ± 0.8	1.5038	3.2
7	S	Ph-Chl	<2	2.80	68.4	4.20	936.9	643.6	17.0 ± 0.7	1.5036	3.1
8	S	Ph-Chl	<2	4.50	67.2	4.79	900.2	430.8	23.8 ± 1.0	1.5038	3.1
9	S	Ph-Chl	<2	2.86	71.6	4.38	1041.0	762.7	16.6 ± 0.7	1.5040	3.3
10A	Ca	Ph-Chl	<2	3.12	60.3	6.40	745.3	617.3	12.4 ± 0.6	1.5075	2.9
10B	Ca	Ph-Chl	<20	3.04	76.0	5.14	1230.0	1056.0	15.1 ± 0.6		
11	Ca	Ph-Chl	<2	2.75	62.0	4.85	778.0	571.2	14.4 ± 0.7	1.5075	2.8
13A	Ca	Ph-Chl	0.6–2	2.33	52.3	5.21	620.1	485.6	11.5 ± 0.7	1.5051	3.1
13A	Ca	Ph-Chl	2–6	2.49	66.5	5.14	992.0	886.7	12.4 ± 0.7		
13A	Ca	Ph-Chl	6–20	2.37	63.5	4.78	814.0	778.4	12.7 ± 0.7		
13B	Ca	Ph-Chl	<20	2.45	68.6	4.94	940.6	871.3	12.6 ± 0.6		
14	Ca	Ph-Chl	<20	2.17	73.0	4.62	1093.0	1137.0	12.0 ± 0.5	1.5043	3.0
20	S	Ph-Chl	<2	3.62	84.7	7.77	1936.0	2353.0	11.9 ± 0.4	1.5059	2.8
20B	Ch	Ph-Chl	<2	3.10	62.2	7.60	781.1	797.4	10.4 ± 0.5	1.5051	2.8
23	C	Ph-Chl	0.6–2	3.86	69.7	7.47	974.0	878.3	13.2 ± 0.6	1.5097	3.1
23	C	Ph-Chl	2–6	4.18	60.0	6.55	714.4	467.6	16.3 ± 0.7		
23	C	Ph-Chl	6–20	5.06	77.2	4.88	1308.0	653.0	26.5 ± 0.9		
30A	Ch	Ph-Chl	<2	1.73	47.6	3.69	536.8	382.0	12.0 ± 0.8	1.5110	2.8
32A	Ch	Ph-Chl	<20	4.27	78.0	5.88	1345.0	966.6	18.5 ± 0.7	1.5110	
32B	Ch	Ph-Chl	<2	2.69	57.2	4.39	691.1	431.2	15.6 ± 0.8	1.5110	3.3
99B	Phy	whole rock	—	3.69	82.2	3.30	1664.0	819.9	28.3 ± 1.0		
99C	Phy	whole rock	—	3.81	83.2	3.18	1761.0	817.5	30.4 ± 1.1		
99C	Phy	mu-chl	<2	2.55	55.1	3.33	658.9	317.4	19.5 ± 1.1	—	3.0
99D	Phy	whole rock	—	3.45	82.3	3.51	1671.0	937.8	24.9 ± 0.9		
99D	Phy	Ph-Chl	<2	3.17	38.1	3.71	477.4	142.5	21.7 ± 1.7	—	2.4
99E	—	vein Qtz	—	25.87	93.4	—	4473.0	0	—		
100A	Phy	whole rock	—	3.03	74.9	2.91	1175.0	565.6	26.4 ± 1.1		
100B	Phy	whole rock	—	4.94	85.4	1.51	2027.0	354.1	81.8 ± 2.9		
100B	Phy	Ph-Chl	<2	4.27	25.4	3.40	396.2	53.70	31.8 ± 3.8	—	2.9
100C	Phy	whole rock	—	4.45	86.1	1.84	2127.0	506.2	60.8 ± 2.1		
100D	Phy	whole rock	—	6.52	91.4	3.61	3436.0	1163.0	45.6 ± 1.5		
100D	Phy	Ph-Chl	<2	5.49	30.3	4.93	424.3	77.44	28.2 ± 2.8	—	2.8
100E	Phy	whole rock	—	4.59	82.2	2.40	1716.0	496.6	48.3 ± 1.7		
100G	—	vein Qtz	—	4.82	91.7	—	3558.0	0	—		

* Sample number. See also site locations in Figs. 1, 2 and in Table 5.
† Rock type: S, slate; Ch, cherty-schist; Ca, calc-schist; Phy, phyllite.
‡ Rock type: WR, whole rock; Mu, muscovite; Ph, phengite; Chl, chlorite; Qtz, synkinematic vein quartz.
§ Size fraction in μm.
‖ Ages calculated using the constants: isotope abundance of $^{40}K = 0.01167$ atom %. $\lambda(^{40}K_c) = 4.962 \times 10^{-10}\,a^{-1}$, $\lambda(^{40}K_c) + \lambda'(^{40}K_c) = 0.581 \times 10^{-10}\,a^{-1}$.

separate, dating method used, and structural style, is presented in Table 1. Conventional K–Ar measurements on both cover and basement are presented in Table 2. The $^{40}Ar/^{39}Ar$ incremental heating results, carried out on 11 samples from the cover, are presented in Table 3. Of the 11 samples dated by the $^{40}Ar/^{39}Ar$ technique, two of these (samples 1 and 23) were measured at three ranges of grain sizes: 0.6–2, 2–6 and 6–20 μm. A duplicate measurement was made on sample 32A. Further conventional K–Ar measurements were made on whole rock specimens and vein quartz from the Paleozoic basement and Permo-Triassic Verrucano rocks. These results are presented in Appendix 1. In the following sections we discuss the results and significance of measurements made in the cover rocks.

The conventional K–Ar dates range from 28 to 10 Ma (Table 2). A quartz-rich chert sample from the cover was analyzed (Table 3) in an attempt to evaluate the extent of excess argon contamination in the cover samples. Its $^{40}Ar/^{36}Ar$ ratio was 380.

Slate results

Four slates (samples 1–4) were collected within an individual exposure where non-penetrative D_{2A} phase crenulations are variably developed (Fig. 3a). In general, apparent K–Ar ages appear to decrease as the degree of crenulation intensifies.

Sample 3 is dominated by a relatively uncrenulated S_1 slaty cleavage defined by the preferred orientation of phengitic white mica and chlorite. The 0.6–2 μm size fraction yields a conventional K–Ar date of 27.0 ± 1.0 Ma. The slaty cleavage of sample 3 is crenulated by

Table 3. $^{40}Ar/^{39}Ar$ analytical data for incremental heating experiments on phengitic white mica, Alpi Apuane area, Northern Apennines, Italy

Release temperature (°C)	$(^{40}Ar/^{39}Ar)^*$	$(^{36}Ar/^{39}Ar)^*$	^{39}Ar % of total	% ^{40}Ar non-atmos.†	Apparent age (Ma)‡
Sample 1 (0.6–2)§; $J = 0.007695$					
450	25.89	0.08799	2.26	3.43	2.6 ± 1.1
470	3.27	0.00578	32.49	47.62	21.5 ± 0.5
485	4.28	0.00870	17.05	39.84	23.5 ± 0.6
500	3.00	0.00344	47.13	65.87	27.2 ± 0.6
Fusion	40.39	0.13475	1.07	1.40	7.8 ± 3.8
Total	4.32	0.00841	100.00	53.31	23.9 ± 1.6
Sample 1 (2–6); $J = 0.008650$					
450	3.99	0.01309	3.05	23.05	13.9 ± 1.6
475	2.25	0.00336	4.55	55.63	18.8 ± 1.4
500	1.89	0.00108	20.99	82.75	23.5 ± 0.6
550	1.98	0.00049	16.16	92.42	27.4 ± 0.7
650	1.82	0.00027	45.40	95.39	26.1 ± 0.6
700	2.00	0.00077	7.95	88.35	26.6 ± 0.8
750	3.47	0.00434	1.23	63.00	32.8 ± 4.0
850	6.19	0.01612	0.45	23.48	21.9 ± 9.0
Fusion	48.70	0.15808	0.21	4.10	29.9 ± 8.0
Total	2.10	0.00141	100.00	86.76	25.2 ± 1.8
Sample 1 (6–20); $J = 0.007955$					
450	11.64	0.03673	7.07	6.67	11.1 ± 1.2
470	4.47	0.00943	18.58	37.48	23.9 ± 0.8
485	3.71	0.00555	34.60	55.63	29.4 ± 0.8
500	4.09	0.00655	27.04	52.49	30.5 ± 0.8
525	9.28	0.02351	7.51	25.06	33.1 ± 2.0
550	25.12	0.07464	2.10	12.19	43.4 ± 8.4
Fusion	36.23	0.11322	3.10	7.64	39.3 ± 3.9
Total	6.39	0.01489	100.00	43.25	28.2 ± 1.4
Sample 13 (2–6); $J = 0.007951$					
450	5.11	0.01528	1.77	11.53	8.4 ± 4.1
475	1.96	0.00426	3.82	35.36	9.9 ± 1.6
500	1.06	0.00122	17.86	65.66	10.0 ± 0.4
550	1.07	0.00054	20.37	84.51	12.9 ± 0.4
600	1.03	0.00034	32.53	89.56	13.2 ± 0.3
650	1.13	0.00061	11.78	83.63	13.5 ± 0.4
750	1.48	0.00120	9.16	75.65	16.0 ± 0.6
Fusion	4.30	0.01052	2.71	27.60	16.9 ± 2.8
Total	1.29	0.00134	100.00	77.16	12.7 ± 0.9
Sample 20 (2–6); $J = 0.007685$					
450	45.38	0.15632	1.15	1.79	2.6 ± 1.9
470	3.08	0.00843	14.92	18.89	8.1 ± 0.5
485	1.80	0.00325	43.56	46.16	11.5 ± 0.3
500	2.06	0.00417	31.63	39.83	11.3 ± 0.4
525	7.11	0.02194	6.06	8.73	8.6 ± 1.8
550	20.45	0.06692	1.81	3.29	9.3 ± 5.2
Fusion	55.57	0.18882	0.88	3.41	3.1 ± 6.1
Total	3.70	0.00999	100.00	36.08	10.3 ± 0.8
Sample 20B (2–6); $J = 0.007962$					
450	4.46	0.01342	0.93	10.93	7.0 ± 4.8
475	2.11	0.00465	1.70	34.61	10.5 ± 2.6
500	1.01	0.00108	21.19	67.96	9.9 ± 0.6
550	0.88	0.00018	13.65	93.46	11.7 ± 0.4
600	0.86	0.00007	30.57	96.92	12.0 ± 0.3
650	0.88	0.00013	17.89	94.88	12.1 ± 0.3
750	1.01	0.00026	12.59	92.05	13.4 ± 0.5
1150	5.16	0.01261	1.49	28.30	20.9 ± 2.4
Total	1.04	0.00072	100.00	86.46	11.7 ± 0.8
Sample 23 (0.6–2); $J = 0.008780$					
450	3.34	0.00941	9.92	16.55	8.7 ± 0.7
475	1.43	0.00297	8.64	38.17	8.6 ± 0.4
485	1.35	0.00116	19.97	74.08	15.7 ± 0.3
500	1.29	0.00076	17.11	82.02	16.6 ± 0.5
510	1.29	0.00075	17.65	82.36	16.8 ± 0.7
525	1.47	0.00053	8.38	88.91	20.5 ± 0.6
535	1.54	0.00101	5.92	80.24	19.5 ± 0.7
550	1.47	0.00079	6.28	83.70	19.4 ± 0.7
600	1.63	0.00111	5.11	79.58	20.4 ± 0.9
750	6.05	0.01277	1.02	37.55	35.6 ± 7.7
Total	1.62	0.00203	100.00	70.21	16.1 ± 0.7

Table 3. Continued

Release temperature (°C)	$(^{40}Ar/^{39}Ar)^*$	$(^{36}Ar/^{39}Ar)^*$	^{39}Ar % of total	% ^{40}Ar non-atmos.†	Apparent age (Ma)‡
Sample 23 (2–6); $J = 0.008415$					
450	5.23	0.01635	2.83	7.45	5.9 ± 1.3
475	1.41	0.00316	5.90	33.27	7.1 ± 0.5
500	1.08	0.00056	27.32	84.10	13.7 ± 0.3
525	1.17	0.00038	20.66	89.84	15.9 ± 0.3
550	1.30	0.00031	21.96	92.46	18.1 ± 0.4
600	1.36	0.00036	13.64	91.80	18.7 ± 0.5
650	1.70	0.00069	5.66	87.68	22.5 ± 0.8
750	3.75	0.00498	1.83	60.57	34.2 ± 1.9
Fusion	52.58	0.46876	0.21	5.15	40.7 ± 17.1
Total	1.51	0.00148	100.00	82.61	16.2 ± 0.9
Sample 23 (6–20); $J = 0.008872$					
450	4.60	0.01468	5.32	5.55	4.1 ± 1.3
475	1.86	0.00382	4.04	38.92	11.6 ± 1.7
485	2.22	0.00368	4.76	50.89	18.0 ± 1.6
500	1.57	0.00128	9.72	75.58	18.9 ± 0.6
510	1.72	0.00142	9.31	75.34	20.6 ± 0.7
525	2.03	0.00133	6.40	80.28	25.9 ± 1.2
535	2.38	0.00198	3.16	75.23	28.5 ± 1.1
550	2.40	0.00253	3.50	68.66	26.2 ± 1.4
600	2.00	0.00088	9.17	86.63	27.5 ± 0.7
650	2.08	0.00059	13.09	91.35	30.1 ± 1.1
750	2.47	0.00082	22.64	89.93	35.2 ± 0.4
Fusion	7.81	0.01170	8.87	55.67	68.3 ± 0.8
Total	2.74	0.00299	100.00	73.78	29.3 ± 1.0
Sample 32A (6–20); $J = 0.008651$					
475	3.24	0.00796	9.29	27.17	13.7 ± 1.0
500	1.45	0.00140	22.30	71.20	16.1 ± 0.4
550	1.42	0.00079	12.76	83.08	18.3 ± 0.5
650	1.72	0.00154	6.85	73.34	19.6 ± 0.9
750	1.37	0.00041	39.83	90.71	19.3 ± 0.4
850	2.23	0.00147	8.18	80.35	27.7 ± 0.8
Fusion	14.01	0.03255	0.79	32.92	70.7 ± 9.0
Total	1.76	0.00180	100.00	76.99	19.1 ± 1.2
Sample 32A (6–20); $J = 0.008355$					
450	4.03	0.01081	6.02	20.57	12.5 ± 0.6
475	1.91	0.00310	6.46	51.83	14.9 ± 0.7
500	1.43	0.00087	31.49	81.57	17.5 ± 0.4
525	1.41	0.00040	24.23	91.12	19.2 ± 0.5
550	1.43	0.00017	16.19	96.17	20.7 ± 0.5
600	1.61	0.00052	9.53	90.10	21.7 ± 0.6
700	2.58	0.00109	5.58	87.34	33.4 ± 1.3
Fusion	28.59	0.07205	0.51	25.51	106.8 ± 12.6
Total	1.83	0.00172	100.00	81.51	19.6 ± 1.07

* Measured.
† $[^{40}Ar_{tot} - (^{36}Ar_{atmos.})(295.5)]/^{40}Ar$ tot.
‡ Calculated using correction factors of Dalrymple *et al.* (1981); $^{37}Ar/^{39}Ar$ corrected ratio less than 0.3 in all analyses; 2σ errors estimates.
§ Concentrate size in μm.

Table 4. Locations of samples in Alpi Apuane region

Site*	Samples	Locality	Map	Location§	
A	1–4	Torrente Acqua Bianca southwest of Gorfigliano	Gorfigliano† (249071)	N = 4 887 275	E = 1 599 150
B	5–9	Arnetola Valley south of Vagli di Sopra	Vagli di Sopra† (249083)	N = 4 883 750	E = 1 600 200
C	10, 11, 23	Arnetola Valley	Vagli di Sopra† (249083)	N = 4 884 150	E = 1 600 125
D	13, 14	Arnetola Valley	Resceto† (249111)	N = 4 883 550	E = 1 599 825
E	20, 21	Col de Beteti, Arnetola Valley	Monte Sumbra† (249124)	N = 4 883 037	E = 1 600 675
F	30	Passo della Focolaccia	Monte Tambura† (249072)	N = 4 884 850	E = 1 597 475
G	32	Monte Cavallo	Monte Tambura† (249072)	N = 4 885 920	E = 1 597 400
H	99	Fiume Frigido, Massa	Massa‡ (Foglio 96)	Roadcut on south side of Fiume Frigido, just northeast of Massa	
I	100	Terrinca	Massa‡ (Foglio 96)	On road from Terrinca to Levigliani	

* Refer to Fig. 1.
† Carta Tecnica Regionale (Regione Toscana) 1:5,000.
‡ Carta topografica (Istituto geografico militare) 1:100,000.
§ Carta Tecnica Regionale grid coordinates.

D_{2A} phase structures in sample 1. Figure 4(a) shows a photomicrograph of the S_1 cleavage in sample 3, relatively unaffected by D_2 crenulations. Three size fractions were prepared from sample 1 for K–Ar and $^{40}Ar/^{39}Ar$ analyses. The <0.6, 0.6–2 and 2–6 μm size fractions yield K–Ar dates of 22.7 ± 0.9, 24.6 ± 0.9 and 24.8 ± 0.9 Ma, respectively. All three size fractions display internally discordant $^{40}Ar/^{39}Ar$ spectra (Fig. 5, Table 3) which define total-gas ages of 23.9 ± 1.6 Ma (0.6–2 μm), 25.2 ± 1.8 Ma (2–6 μm) and 28.2 ± 1.4 Ma (6–20 μm). D_{2A} crenulations are more strongly developed in samples 4 and 2 collected at this same location (Figs. 3a and 4b); K–Ar dates of 21.9 ± 0.9 Ma and 14.2 ± 0.6 Ma are recorded in the <2 μm size fractions separated from these two samples, respectively.

In another locality where slates are variably crenulated (location B, Table 4, Fig. 1), a similar decrease in K–Ar age with increase in degree of crenulation development was observed. The 0.6–2 μm size fraction of white micas separated from five samples yield K–Ar ages between 23.8 ± 1.0 Ma and 16.6 ± 0.7 Ma, with younger dates systematically recorded in the more crenulated slates.

A slate sample with a penetrative differentiated D_3 crenulation cleavage was collected at site C (Fig. 1). Phengites were mechanically scraped off D_3 cleavage planes and several size fractions were prepared. These record the following K–Ar dates: 13.2 ± 0.6 Ma (0.6–2 μm), 16.3 ± 0.7 Ma (2–6 μm) and 26.5 ± 0.9 Ma (6–20 μm). Each size fraction was also analyzed with $^{40}Ar/^{39}Ar$ incremental heating technique. All display internally discordant age spectra which yield the following total gas ages (Fig. 6, Table 3): 16.0 ± 0.6 Ma (0.6–2 μm), 16.2 ± 0.9 Ma (2–6 μm), and 29.3 ± 1.0 Ma (6–20 μm).

Slate sample 20 collected at site E (Fig. 1) consists of S_1 phengites which have been severely crenulated during the D_{2A} phase. A K–Ar age of 11.90 ± 0.4 Ma is recorded by the 0.6–2 μm size fraction. The 2–6 μm size fraction from this sample displays an internally discordant, $^{40}Ar/^{39}Ar$ spectrum which defines a total-gas age of 10.3 ± 0.8 Ma (Fig. 7, Table 3). A plateau age of 11.5 Ma is defined by the intermediate temperature gas fraction evolved from this sample.

The slate results may be summarized as follows: (1) K–Ar ages decrease as the extent of crenulation increases; (2) for individual samples, K–Ar ages decrease as grain size decreases; (3) for individual samples, the character of $^{40}Ar/^{39}Ar$ release spectra varies according to grain size analyzed, with the finer grain sizes yielding more nearly concordant results; and (4) phengites associated with D_1 phase structures yield generally greater ages than phengites associated with younger structures. The significance of these observations is discussed in a subsequent section.

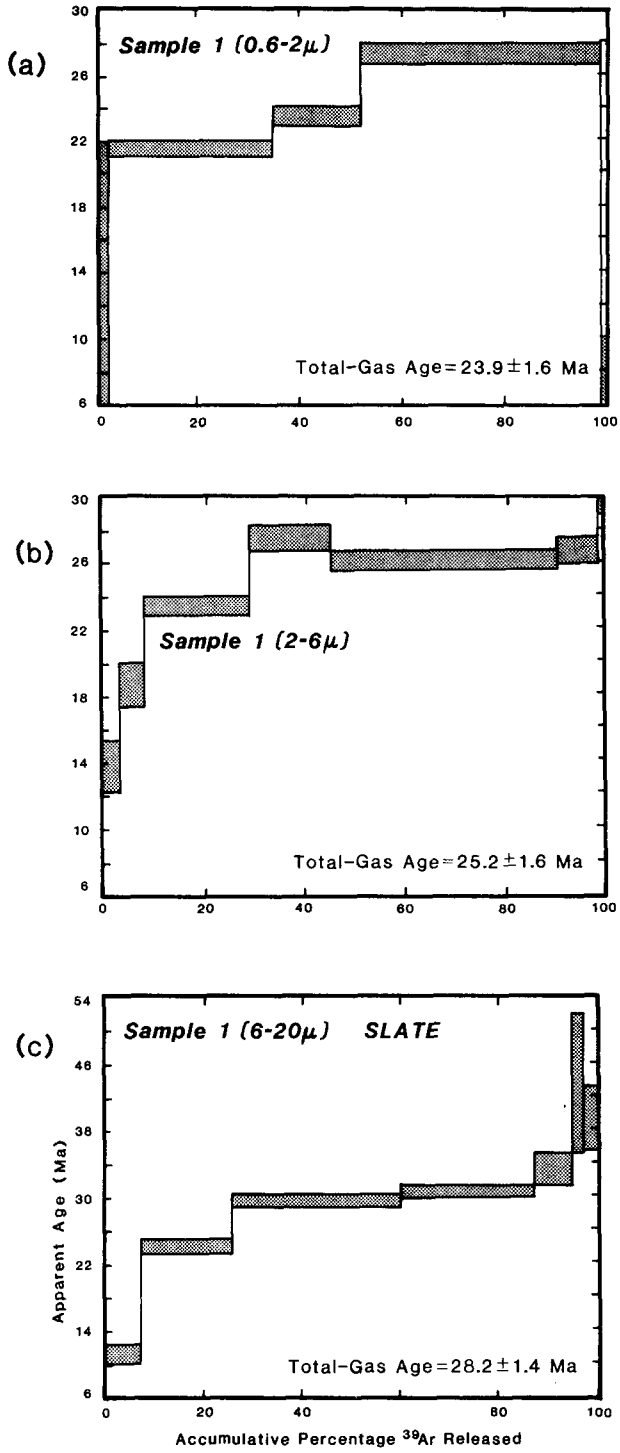

Fig. 5. $^{40}Ar/^{39}Ar$ Incremental heating release patterns in slate sample 1. Increasingly higher release temperatures up to fusion from left to right. Estimated uncertainties (2σ) indicated by width of bar. (a) 0.6–2 μm size fraction; (b) 2–6 μm and (c) 6–20 μm.

Results from cherty schists

Exposures of cherty schists which typically consist of alternating layers of chert-rich and phyllitic layers display a well-developed S_1 foliation defined by aligned phengite and chlorite (Figs. 3b and 8). In exposures affected by D_{2A} and/or D_3 phase deformation, little crenulation of the S_1 foliation is seen within chert layers and there appears to be no crystallization of S_2 or S_3 white micas (Fig. 8a). However, penetrative S_{2A} or S_3 foliations are found within the interbedded phyllite horizons, where it appears that in addition to physical rotation of earlier formed grains of phengite and chlorite,

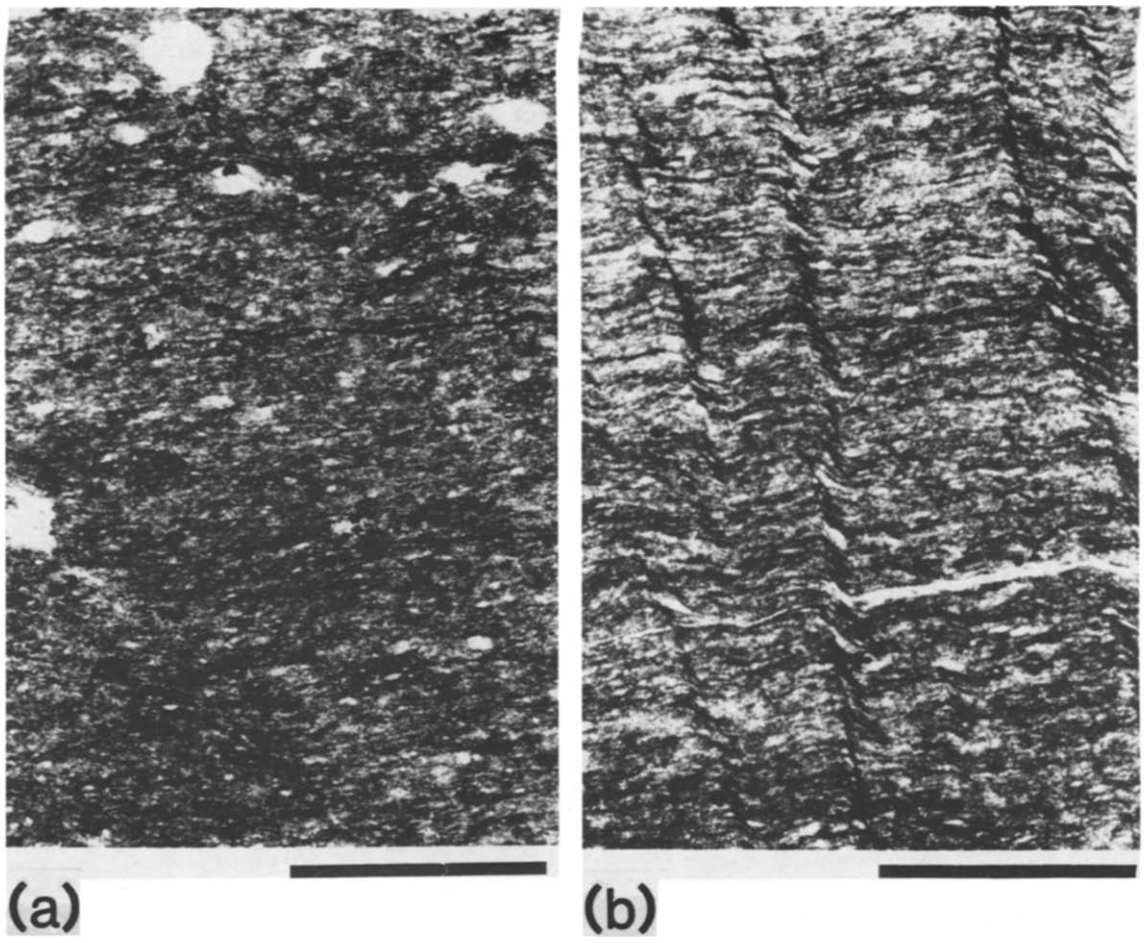

Fig. 4. Effect of progressive crenulation on the S_1 mica structures in slates at site A (Fig. 3a). Scale bars are 0.5 mm. The K–Ar ages in the fine fraction separates decrease as the intensity of crenulation becomes greater. (a) Sample 1; (b) Sample 4.

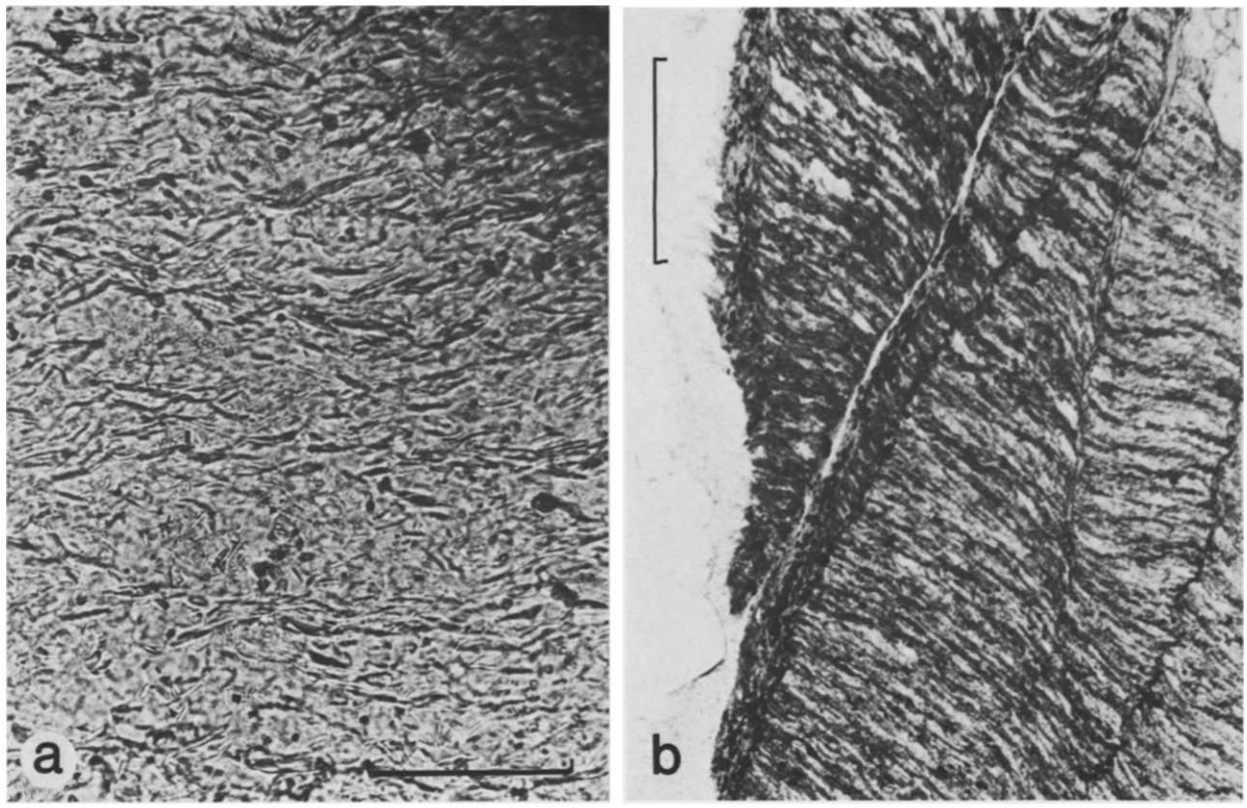

Fig. 8. Variation in structural development of D_2 phengites at site G (Fig. 3b). (a) Sample 32B consists of S_1 phengites which are structurally unfolded by the later deformation phase. (b) Sample 32A consists of material physically separated from the surface of a typical strain slip cleavage of the D_2 phase. 32A from phyllite layer and 32B from chert layer. Scale bars are 0.5 mm.

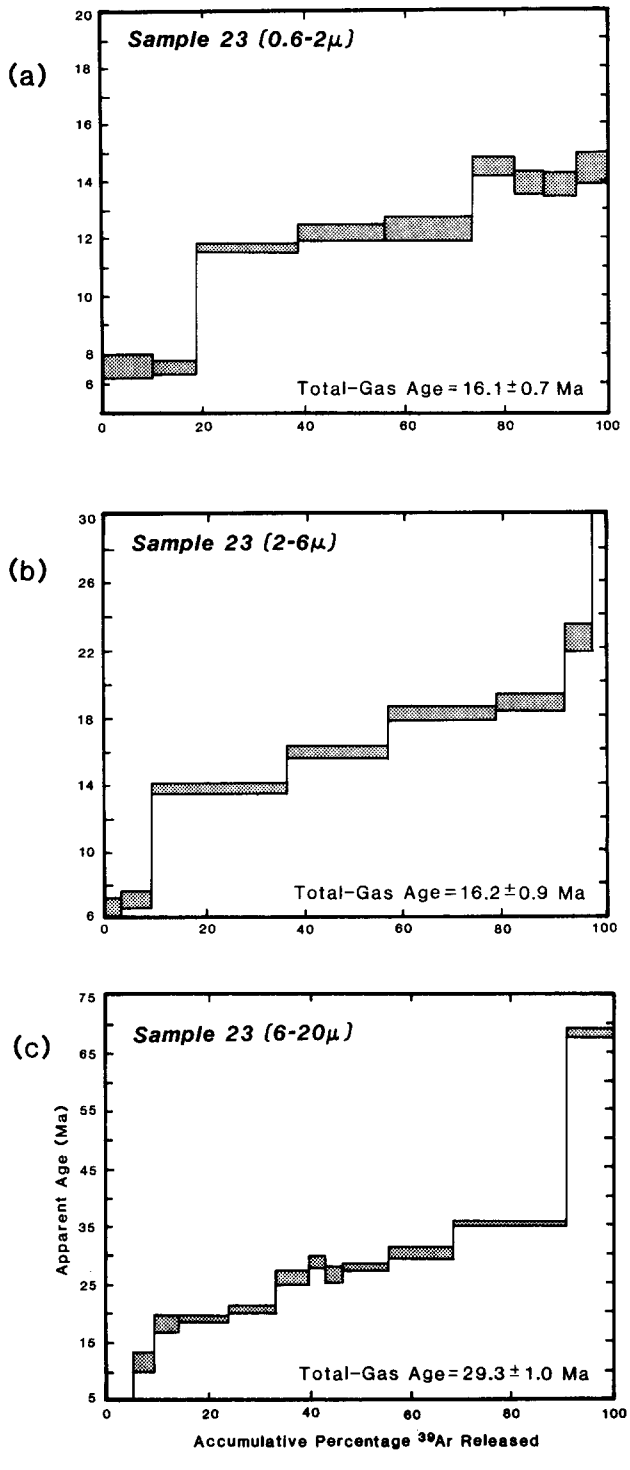

Fig. 6. Effect of grain size on $^{40}Ar/^{39}Ar$ incremental heating release spectra in phengite from slate number 23. (a) 0.6–2 μm size fraction; (b) 2–6 μm and (c) 6–20 μm.

new crystals of both minerals have formed along the secondary cleavage surfaces (Fig. 8b). These new grains are distinctly larger than the earlier formed S_1 grains ranging in size from 6 to 20 μm. In addition, smaller (<2–6 μm) randomly oriented grains of chlorite and phengite are present in both the chert and phyllite layers.

A chert sample (20B) was collected adjacent to the slate sample (20) previously discussed (site E). It contains generally uncrenulated S_1 phengite and chlorite which is overgrown by a subordinate amount of ran-

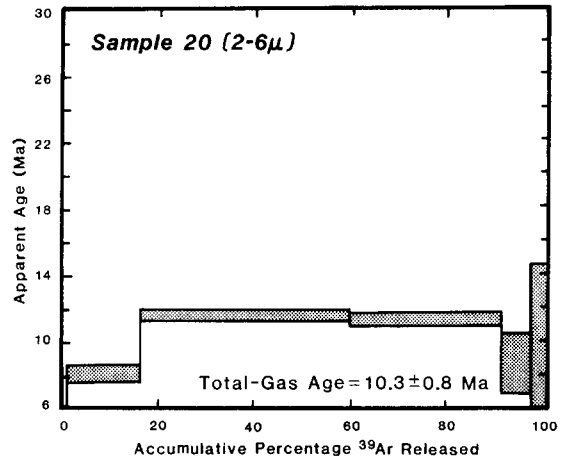

Fig. 7. $^{40}Ar/^{39}Ar$ Incremental heating release spectra in crenulated phengite, (sample 20) 2–6 μm size fraction.

domly oriented phengite and chlorite grains. A K–Ar age of 10.4 ± 0.5 Ma was determined for the 0.6–2 μm size fraction from this sample. $^{40}Ar/^{39}Ar$ analysis of the 2–6 μm size fraction yields an internally discordant spectrum (Fig. 9, Table 3) with a total-gas age of 11.7 ± 0.8 Ma. A plateau age of 12.0 Ma is defined by the intermediate temperature gas fractions evolved from this sample.

Two samples were collected from a cherty schist displaying similar structures at site G (Fig. 1). Here the 0.6–2 μm size fraction of phengite within an undeformed chert clast (32B in Fig. 8a) yields a K–Ar date of 15.6 ± 0.8 Ma. Phengites were scraped off a penetrative D_{2A} differentiated crenulation cleavage within an adjacent phyllite layer (Fig. 8b). This material (32A) appears to consist largely of relatively coarse-grained S_{2A} phengite together with subordinate amounts of smaller sized S_1 phengite. The <20 μm size fraction of this material records a K–Ar age of 18.5 ± 0.7 Ma. A portion of the 2–20 μm size fraction was analyzed in duplicate by $^{40}Ar/^{39}Ar$ methods. It displays an internally discordant age spectra with total-gas ages of 19.1 ± 1.2 and 19.6 ± 1.0 Ma (Table 3, Fig. 9).

Results from calc-schists

S_1 foliations within most exposures of calc-schist are complexly deformed by D_{2A} and/or D_3 folds with a general development of attendant secondary fabric elements (Fig. 3). K–Ar ages of the 0.6–2 μm size fraction of calc schist samples are 12.40 ± 0.6 Ma (sample 10), 14.4 ± 0.7 Ma (11) and 12.9 ± 0.5 Ma, for samples 10, 11 and 14, respectively. The 2–20 μm size fraction of sample 10 yield a slightly older K–Ar date of 15.1 ± 0.6 Ma (Table 2).

Sample 13 is characterized by penetrative development of both D_{2A} and D_3 crenulations of the S_1 foliation. This sample was selected for more detailed size analyses. The following K–Ar dates were determined: 11.5 ± 0.7 Ma (0.6–2 μm); 12.4 ± 0.7 Ma (2–6 μm); and 12.7 ± 0.7 Ma (6–20 μm) (Table 2). A $^{40}Ar/^{39}Ar$ incremental-heating experiment was carried out on a portion of the

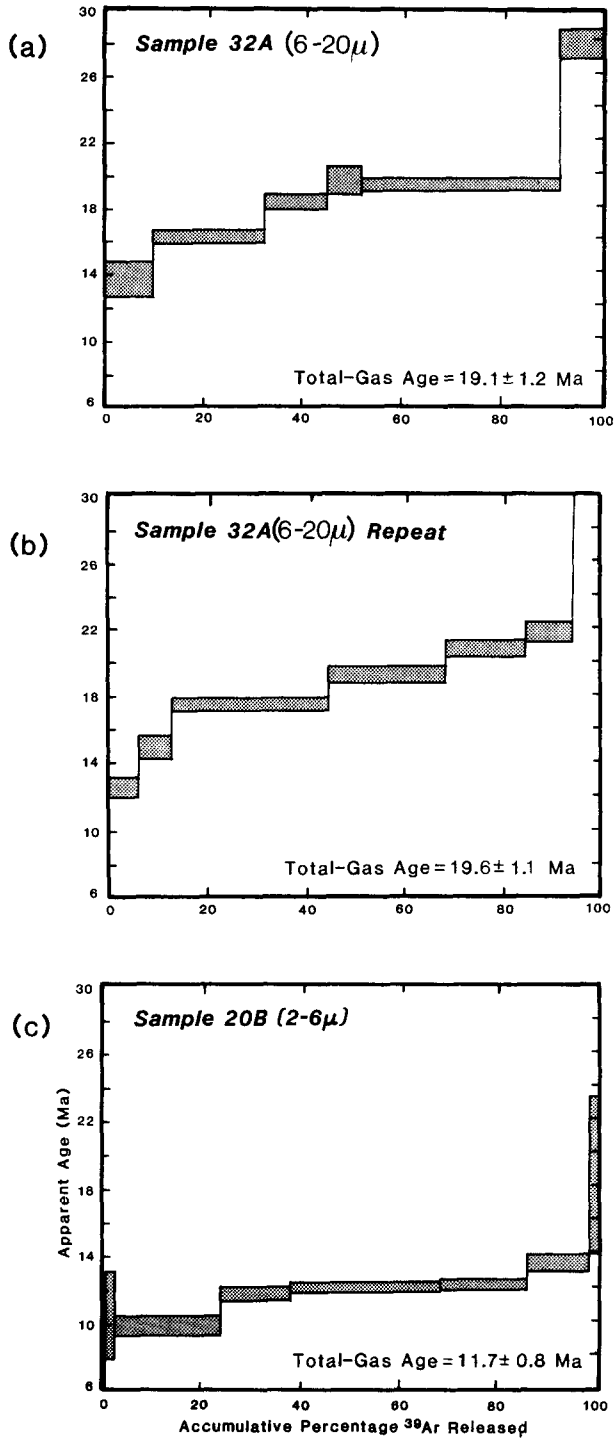

Fig. 9. $^{40}Ar/^{39}Ar$ Incremental heating release spectra in chert schists. Sample 32 is shown after repeat measurement.

2–6 μm size fraction from sample 13. This material displays an internally discordant age spectrum with a total-gas date of 12.7 ± 0.9 Ma (Table 3; Fig. 10). A plateau age of *c.* 13.2 Ma is defined by intermediate-temperature gas fractions evolved from the sample.

INTERPRETATION

K–Ar and $^{40}Ar/^{39}Ar$ dates ranging between 28 and 10 Ma have been obtained from fine-grained size fractions of phengite prepared from rocks within cover tectonic units in the Alpi Apuane. Although variable, the dates are consistent with regional stratigraphic brackets on the possible age of Tertiary tectonothermal activity recorded in the area. The analyzed samples were chosen in an attempt to isolate and date phengites associated with the various structural phases described from the Northern Apennines. The results allow for reasonable geochronologic calibration of the deformational history.

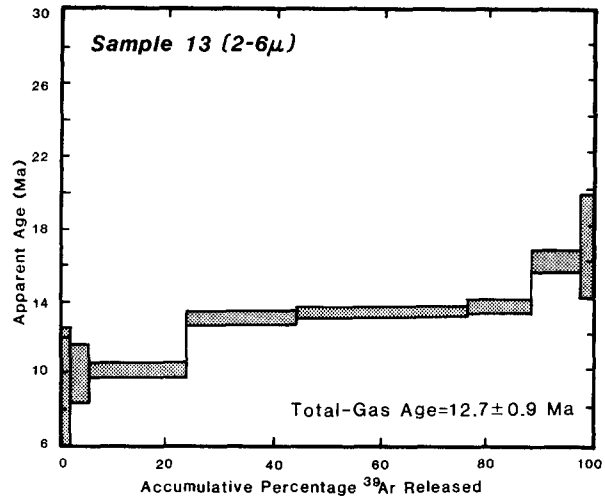

Fig. 10. $^{40}Ar/^{39}Ar$ Incremental heating release spectrum in calc schist at site D.

Age of D_1 *foliation*

The oldest K–Ar dates (27.0–23.8 Ma) have been obtained from slate samples (1, 3, 8) characterized by uncrenulated S_1 phengite. $^{40}Ar/^{39}Ar$ age spectra of three fine-grained size fractions from one of these samples (1) display a mutually similar pattern of internal discordance with apparent ages systematically increasing throughout low-temperature portions of the analyses. Intermediate- and high-temperature gas fractions evolved from the 2–6 μm and 0.6–2 μm size fractions record very similar dates of 26.5–27.0 Ma, which probably closely date formation of the S_1 foliation. A slighly older date of *c.* 30 Ma is defined by the intermediate-temperature gas fractions evolved from the coarser-grained 6–20 μm size fraction. The older date probably reflects a contribution of ^{40}Ar from subordinate detrital mica in this coarser grained size fraction.

The nature of $^{40}Ar/^{39}Ar$ spectra discordancy displayed by the three size fractions of sample 1 appears to characterize intracrystalline isotopic systems which have experienced partial volume diffusive loss of radiogenic ^{40}Ar as a result of a post-crystallization thermal disturbance (e.g. Turner 1970, Dallmeyer 1975, Harrison 1981). Ages recorded by low-temperature gas fractions evolved from the various size fractions of sample 1 suggest this thermal disturbance may have occurred at *c.* 12–14 Ma. The finer-grain size fractions appear to have lost relatively greater amounts of radiogenic argon and record the youngest $^{40}Ar/^{39}Ar$ total-gas dates. The

chronologic relationship between the apparent post-crystallization disturbance and later deformational events is uncertain. Systematically younger K–Ar dates (down to 14.2 Ma) are recorded by the more penetratively crenulated (D_{2A} phase) slate samples collected from the same exposure. However, it is not likely that such small-scale thermal gradients could have been maintained during development of D_2 strains. Perhaps mechanical flexing of the small phengite grains within the relatively high-strain crenulation zones resulted in an increase in the density of lattice dislocations. This could have rendered grains within these zones more susceptible to diffusive loss of radiogenic argon during the syntectonic maintenance of middle greenschist facies regional metamorphic conditions. This interpretation may be supported by results of the isotopic analyses of material scraped off D_{2A} differentiated crenulation cleavages in a phyllite horizon within an exposure of cherty schist (sample 32A). Duplicate $^{40}Ar/^{39}Ar$ analyses of the 2–20 μm size fraction of this material yields internally discordant age spectra of generally similar character to those of sample 1. Once again, apparent ages systematically rise from initial values of *c.* 12–14 Ma over low-temperature gas fractions. However, in contrast to the spectrum of sample 1, intermediate- and high-temperature plateaus are not defined in sample 32A, and the apparent ages rise throughout the analysis, approaching *c.* 27 Ma only in the fusion increment. This more extensive spectral discordance may reflect a significantly greater loss of radiogenic argon from initial S_1 phengites during their collapse and rotation into the D_{2A} differentiated crenulation cleavage (at 12–14 Ma?).

Age of D_2 *foliation*

Insight into the chronology of D_{2A} strain may be gained by results of the isotopic analyses of samples 20 and 20B collected within an exposure of cherty schist. Sample 20 is an intensely crenulated phyllite (D_{2A} generation) with a penetrative S_2 surface defined by both rotated S_1 and neomineralized S_2 micas. In addition, this surface is locally overgrown by smaller, post-tectonic phengite. The 0.6–2 μm size fraction of the phyllite records a K–Ar date of 11.9 ± 0.4 Ma. The 2–6 μm size fraction yields an internally discordant $^{40}Ar/^{39}Ar$ spectrum; however, an intermediate-temperature age plateau of *c.* 11.5–12 Ma is well defined. The low-temperature gas increments record slightly younger dates of *c.* 8–10 Ma. Sample 20B is an undeformed chert clast collected adjacent to the sample 20 phyllite. It contains undeformed S_1 phengite which are locally overgrown by a few grains of randomly oriented phengite and chlorite microporphyroblasts. The 0.6–2 μm size fraction of this material yields a K–Ar date of 10.4 ± 0.5 Ma. The 2–6 μm size is characterized by an internally discordant $^{40}Ar/^{39}Ar$ age spectrum; however once again, intermediate-temperature gas fractions yield a *c.* 11.5–12 Ma plateau. Younger dates of *c.* 10 Ma are also recorded by the low-temperature gas fractions. The argon characteristics of these two samples suggest that a date of *c.* 12 Ma may be appropriate for development of D_{2A} strains and the apparently concomitant partial resetting of crenulated S_1 mica grains. The *c.* 8–10 Ma dates seen in low-temperature gas fractions evolved from the two samples may relate to later growth of the small, post-tectonic white mica grains. This latter age is consistent with the available stratigraphic constraints outlined earlier.

A very similar chronology emerges from the analytical results obtained from sample 13 collected within a complexly deformed exposure of calc-schist. Here S_1 micas are bent, broken, and isoclinally folded by both D_{2A} and D_3 crenulations. These cleavages are also characterized by extensive new growth of both D_{2A} and D_3 phengites. The 0.6–2 μm size fraction of this material yields a K–Ar date of 11.4 ± 0.7 Ma. The 2–6 μm size fraction records an internally discordant $^{40}Ar/^{39}Ar$ age spectra, with low-temperature gas fractions yielding apparent dates of *c.* 8–10 Ma, while a plateau of *c.* 12–12.5 Ma is defined by the intermediate-temperature fractions. These results are in harmony with the data discussed above, and suggest that D_{2A} (and perhaps D_3) strains probably developed at *c.* 12 Ma. Argon systems appear to record a distinctly later event at *c.* 8–10 Ma.

Age of D_3 *foliation*

In an effort to more clearly date D_3 deformation, micas were scraped off D_3 spaced cleavage surfaces within slate sample 23. Three different size fractions yield K–Ar dates ranging from 26.5 to 13.2 Ma. Generally similar $^{40}Ar/^{39}Ar$ total-gas dates were obtained for the respective size fractions, although very discordant spectra are displayed. That of the coarsest size fraction (6–20 μm) systematically increases from an initial, low-temperature age of *c.* 8 Ma to *c.* 27–28 Ma in intermediate-temperature fractions. The two highest temperature gas fractions yield markedly older dates. This pattern of age variation suggests that most of the 6–20 μm size fraction along the D_3 spaced cleavage represents an insoluble residue made up predominantly of S_1 micas together with a small percentage of relatively refractory detrital grains. The two smaller size fractions (2–6 μm and <2 μm) also record *c.* 8 Ma dates in low-temperature gas fractions, while apparent ages continue to rise throughout $^{40}Ar/^{39}Ar$ incremental-release analyses to maxima of *c.* 20 Ma (0.6–2 μm) and 24 Ma (2–6 μm). Apparently these phengite size fractions consist of grains which initially formed along an S_1 foliation and were thoroughly outgassed during their subsequent rotation into alignment along the D_3 pressure solution cleavage. The *c.* 8 Ma dates recorded in low-temperature gas fractions are more likely to be related to regional growth of post-tectonic micas than to formation of the D_3 surface.

Summary: ages of the deformation phases

The K–Ar and $^{40}Ar/^{39}Ar$ data reported for fine-grained phengite/muscovite size fractions concentrated

from various units in the cover sequence of the Alpi Apuane provide the following chronologic brackets.

(1) A regional S_1 foliation appears to have developed during a major folding event which occurred at *c.* 27 Ma and was coincident with attainment of lower to middle greenschist facies regional metamorphic conditions.

(2) D_{2A} and D_3 structures are only locally developed and appear to have formed at *c.* 12 Ma. Where penetrative crenulations of S_1 developed, partial resetting of S_1 mica argon systems was accomplished.

(3) Post-tectonic growth of randomly oriented, white mica microporphyroblasts apparently occurred at *c.* 8–10 Ma.

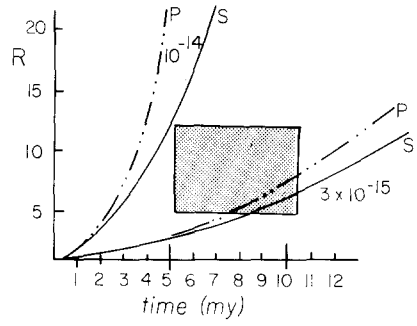

Fig. 11. Geologic strain rate diagram for Alpi Apuane metasediments shown as maximum:minimum strain ratio (R) against time. The solid lines and dashed lines indicate the build up of finite strain through time for displacement processes of simple shear (S) and pure shear (P), respectively (modified from Pffifner & Ramsay 1982, fig. 7). The box indicates the range of finite strain ratios and duration of deformation phase D_1 based on results reviewed in text. Strain rate curves are given in units of s^{-1}.

DISCUSSION

Conventional K–Ar *data*

We have shown that a direct relationship exists between micas associated with different structural phases and apparent K–Ar ages. Purdy & Jäger (1976) indicated that 350 ± 50°C is a reasonable blocking temperature for white mica which cooled from amphibolite facies conditions in the Lepontine region of the Alps. Frey *et al.* (1976) have shown that even at temperatures of as high as 450°C, pre-Alpine muscovites were not completely *rejuvenated* during the Alpine greenschist facies overprint in the Mt. Rosa area. They concluded that not only temperature, but also the degree of Alpine deformation were important factors in the rejuvenation process. In the Alpi Apuane region, temperatures of around 350–400°C and pressures of 3–4 kbar were maintained during all Tertiary deformation phases. The maximum temperature reached during metamorphism was therefore low enough to allow micas formed during the D_1 phase to at least partially survive (i.e. not be completely rejuvenated). The maximum measured age of 27 Ma, associated with D_1 structures, is close to the maximum age allowed by available stratigraphic–paleontologic constraints (between 29 and 8 Ma), and suggests that in certain favorable cases the age of earliest-formed micas may be preserved.

TECTONIC IMPLICATIONS

Strain rates and the length of deformation phases

The K–Ar and $^{40}Ar/^{39}Ar$ dates presented here suggest that metamorphism and deformation within this portion of the Northern Apennines began at *c.* 27 Ma (Late Oligocene) and was terminated by 10–8 Ma (Late Miocene). If the entire sequence of deformation pulses (D_1–D_3) is regarded as a progressive deformation of the Northern Apennine continental margin, then the total strain record must have developed during 15 Ma (difference between the ages of micas associated with the D_1 and D_3 phases).

The finite strains throughout the metamorphic region of the Alpi Apuane have been measured from study of the deformed shapes of the marble breccias, reduction spots, and oncalites (Kligfield *et al.* 1981). Results indicate that strain ratios of from 4.0 to 12.5:1 with average values of 7.0:1 resulted during the polyphase deformation. It was maintained (Kligfield *et al.* 1981) that these strains accumulated primarily during D_1 deformation phase and that subsequent shape change during D_{2A} and D_3 phases was of only minor importance. If only half of the available 15 Ma time span was used for this strain accumulation, then the duration of the D_1 phase would have been approximately 7 Ma. This is in agreement with estimates of 5 Ma for the average duration of deformation events as compiled from a worldwide data base by Pffifner & Ramsay (1982).

The K–Ar and $^{40}Ar/^{39}Ar$ ages allow us to estimate the strain rates which accompanied deformation in the Alpi Apuane region. As shown by Pffifner & Ramsay (1982), a simple division of finite strain by length of deformation phase is not appropriate for this calculation due to the non-linear strain build up with time for different displacement processes (i.e. simple shear versus pure shear). Figure 11 illustrates graphs of strain ratio (R) vs time for differing strain rates (modified from fig. 7 in Pffifner & Ramsay 1982). Located on the graph is the range of Alpi Apuane strain and age values which result from integrating the strain data of Kligfield *et al.* (1981) over time periods of from 10 to 5 Ma. The resultant strain rates vary between 10^{-14} and 10^{-15} s^{-1} *regardless* of whether these strains accumulated by processes of simple shear or by pure shear. Under the 350–400°C temperatures conditions which prevailed, these strain rates are consistent with the ductile deformation processes for the lithologies involved.

Constraints on plate tectonic models

Many workers have suggested that the Tertiary tectonothermal activity recorded in the Northern Apennines is related to rotation of the Corsica–Sardinia microplate away from France and its subsequent collision with the Italian–Adriatic continental margin (Boc-

caletti *et al.* 1971). Geochronological data presented here imply that if the Northern Apennine orogeny was related to collision of Corsica with Italy, this rotation must have initiated prior to at least *c.* 27 Ma. The implications of this chronology for the overall history of microplate interactions in the western Mediterranean and generation of calcalkaline volcanism in Sardinia have been reviewed elsewhere (Kligfield 1980).

Acknowledgements—We thank Professor E. Jäger and members of the isotope geology group at the Mineralogisch-Petrographisches Institut, Universität Bern, for extending laboratory facilities during the early stage of this project and for useful discussions. Drs W. Alvarez, M. Frey, G. Giglia, R. K. O'Nions and S. Carter provided critical reviews of an earlier (1978) version of the manuscript. We thank Drs L. Carmignani, G. Giglia, L. Dallan-Nardi, R. Nardi, and other members of the Instituto de Geologia, Universitá di Pisa, for their hospitality and assistance with fieldwork. The work was financially supported (1972–1978) by U.S. National Science Foundation grants DES 73-0663, EAR 76-84320, EAR 77-1300 (RK); by DES 72-01453-A01 (SS); and by the Swiss National Science Foundation (JH 1972–1982; RK 1978–1981). Partial travel expenses for fieldwork (RDD) were provided by the Swiss National Science Foundation.

APPENDIX 1

Results from the Paleozoic basement and Massa unit

Whole rock ages of phyllites and slates range from 80 to 24 Ma. These samples have $^{40}Ar/^{36}Ar$ ratios that range from 1175 to 3436 (Table 3). The syntectonic vein quartz at sites 100 and 99 have large quantities of radiogenic argon (Table 2) and high $^{40}Ar/^{36}Ar$ ratios of 3558 and 4473, respectively.

The ages of these samples are unreasonable based on available geologic criteria. The age of metamorphism cannot be older than the depositional age of the pseudomacigno (34–29 Ma as previously discussed). The 100 series of Paleozoic age must have been involved in the Hercynian orogeny, since Borsi *et al.* (1967) report a 275 Ma Rb–Sr isochron age from lithologically analogous Paleozoic schists in the nearby Mt. Pisani region to the South, and can be explained by partial resetting to Oligocene–Miocene metamorphic conditions and/or excess argon included during this metamorphism.

For the 99 series, whose sediments were not deposited until after the Hercynian orogeny (Fig. 2), the incorporation of excess argon released from the basement during the Oligocene–Miocene metamorphism as well as partially reset detrital Hercynian micas need an explanation. The large quantities of radiogenic argon measured in the syntectonic vein quartz at sites 100 and 99 (Table 2) suggest large quantities of radiogenic argon released during the Tertiary, present in the fluid phase, and incomplete outgassing of argon from the total rock system of the basement and the Massa unit during the time of Tertiary metamorphism.

The low temperature argon release of the quartz during laboratory heating strongly suggests that the argon is contained in fluid inclusions, a result further supported by analyses of the $<2\ \mu m$ size fraction of the same samples. The measured ages are significantly lower, reflecting the fact that the $<2\ \mu m$ fraction is below the size of the fluid inclusions containing the excess argon. However since the initial $^{40}Ar/^{36}Ar$ ratio in the fluid inclusions was high during Tertiary metamorphism, we cannot rule out the possibility that the $<2\ \mu m$ micas also have incorporated some inherited argon, and their K/Ar ages (99 and 100 fine fraction) may be unreliable and thus are not incorporated into further consideration.

REFERENCES

Ahrendt, H., Hunziker, J. C. & Weber, K. 1977. Age and degree of metamorphism and time of nappe emplacement along the southern margin of the Damara orogen/Namibia (SW-Africa). *Geol. Rdsch.* **67**, 719–742.

Ahrendt, H., Hunziker, J. C. & Weber, K. 1978. K/Ar-Altersbestimmungen an schwach-metamorphen Gesteinen des Rheinischen Schiefergebirges. *Z. dt. geol. Ges.* **129**, 229–247.

Alexander, E. C., Jr., Michelson, G. M. & Lanphere, M. A. 1978. MMhb—1. A new $^{40}Ar/^{39}Ar$ dating standard. In: *Short papers on the Fourth International Conference on Geochronology, Cosmochronology and Isotope Geology* (edited by Zartman, R. A.). *Open File Rep. U.S. Geol. Surv.* **78-701**, 6–8.

Bagnoli, G. & Tongiorgi, M. 1979. New fossiliferous Silurian (Mt. Corchia) and Devonian (Monticiano) layers in the Tuscan Paleozoic. *Mem. Soc. Geol. It.* **20**, 301–313.

Barberi, R. & Giglia, G. 1965. La serie scistosa basale dell' autoctono delle Alpi Apuane. *Boll. Soc. Geol. It.* **84**, 41–92.

Blow, W. H. 1969. Late Middle Eocene to Recent planktonic foraminiferal biostratigraphy. In: *Proc. First International Conference Planktonic Microfossils* (edited by Bronnimann, P. and Renz, H.), Geneva. **1**, 199–421.

Boccaletti, M., Elter, P. & Guazzone, C. 1971. Plate tectonic models for the development of the Western Alps and Northern Apennines. *Nature Lond.* **234**, 108–111.

Borradaile, G. J., Bayly, M. B. & Powell, C. M. (editors) 1982. *Atlas of Deformational and Metamorphic Rock Fabrics*. Springer, New York.

Borsi, S., Ferrara, G., Rau, A. & Tongiorgi, M. 1967. Determinazioni col metodo Rb/Sr dell filladi e quartziti listate di Buti (Monti Pisani). *Atti Soc. Tosc. Sc. Nat., Mem. Ser. A* **73**, 632–646.

Carmignani, L. & Giglia, G. 1975. Aperçu sur la geologie des Apuane: les Unites tectoniques et les grandes structures. *Bull. Soc. Geol. Fr.*, 7 *Ser.* **17**, 963–978.

Carmignani, L. & Giglia, G. 1977. Le fasi tettoniche terziare dell' Autoctono delle Alpi Apuane: studio delle strutture minori della zona centro-meridionale. *Boll. Soc. geol. It.* **94**, 1957–1981.

Carmignani, L. & Giglia, G. 1979. Large scale reverse "drag folds" in the late Alpine building of the Apuan alps (N. Apennines). *Atti Soc. tosc. sci. nat. Mem. Ser.* **A86**, 109–125.

Carmignani, L., Giglia, G. & Kligfield, R. 1978. Structural evolution of the Apuane Alps: an example of continental margin deformation in the Northern Apennines, Italy. *J. Geol.* **86**, 487–504.

Crisci, G., Leoni, L. & Sbrana, A. 1975. La formazione dei marmi delle Alpi Apuane (Toscana). Studio petrografico, mineralogico, e chimico. *Atti soc. Tosc. Sci. Nat. Mem. Sér.* **A82**, 199–236.

Curry, D. & Odin, G. S. 1982. Dating of the Paleogene. In: *Numerical Dating in Stratigraphy* (edited by Odin, G. S.). Wiley, New York.

D'Albissin, M. 1963. *Les traces de la deformation dans les roches calcaires. Revue Géogr. phys. Géol. dyn.* Deux. serie, Fasc. supplementaire.

Dallan-Nardi, L. 1977. Segnolazione di Lepidocycline nelle parte basale dello "pseudomacigno" delle Alpi Apuane. *Boll. Soc. Geol. It.* **95**, 459–477.

Dallan-Nardi, L. & Nardi, R. 1974. Schema stratigrafico e strutturale dell'Appennino settentrionale. *Mem. Acc. Lunig. Sci.* **42**, (1972) 1–212.

Dallmeyer, R. D. 1974. $^{40}Ar/^{39}Ar$ Incremental release ages of biotite and hornblende from pre-Kenoran gneisses between the Matagami–Chibougamau and Frotet–Troilus greenstone belts, Quebec. *Can. J. Earth Sci.* **11**, 1586–1593.

Dallmeyer, R. D. 1975. $^{40}Ar/^{39}Ar$ ages of biotite and hornblende from a progressively remetamorphosed basement terrane: their bearing on interpretation of release spectra. *Geochim. cosmochim. Acta* **39**, 1655–1669.

Dallmeyer, R. D. 1979. $^{40}Ar/^{39}Ar$ dating: principles, techniques, and applications in orogenic terraines. In: *Lectures in Isotope Geology*, (edited by Jager, E. and Hunziker, J. C.). Springer, Berlin, 77–104.

Dallmeyer, R. D. & Rivers, T. 1983. Recognition of extraneous argon components through incremental-release $^{40}Ar/^{39}Ar$ analysis of biotite and hornblende across the Grenvillian metamorphic gradient in southwestern Labrador. *Geochim. cosmochim. Acta* **47**, 413–428.

Dalrymple, G. B. & Lanphere, M. 1969. *Potassium–Argon Dating: Principles, Techniques and Applications to Geochronology*. Freeman & Co., San Francisco.

Dalrymple, G. B. & Lanphere, M. A. 1971. $^{40}Ar/^{39}Ar$ Technique of K–Ar dating: a comparison with the conventional technique. *Earth Planet. Sci. Lett.* **17**, 300–308.

Dalrymple, G., Alexander, E., Lanphere, M. & Kraker, G. 1981. Irradiation of samples for $^{40}Ar/^{39}Ar$ dating using the Geological Survey TRIGA reactor. *Prof. Paper U.S. Geol. Survey* 1176.

Elter, P., Giglia, G., Tongiorgi, M. & Trevisan, L. 1975. Tensional and compressional areas in the recent (Tortonian to present) evolution of the Northern Apennines. *Boll. Geofis. Teor. Appl.* **42**, 3–18.

Federici, P. 1973. La tettonica recente dell'Appennino—I. Il bacino villafranchiano di Sarzana e il suo significato nel quadro dei movimenti distensivi a nord-ovest delle Alpi Apuane. *Boll. Soc. geol. It.* **92**, 287–301.

Frey, M. 1969. Die metamorphose des Keupers vom Tafeljura bis zum Lukmanier-Gebiet. *Beitr. Geol. Karte Schweiz* N.F. **137**, 1–160.

Frey, M. 1978. Progressive low grade metamorphism of a black shale formation, central Swiss Alps, with special reference to pyrophyllite and margarite bearing assemblages. *J. Petrology* **5**, 95–135.

Frey, M., Hunziker, J. C., O'Neil, J. R. & Schwander, H. W. 1976. Equilibrium–disequilibrium relations in the Monte Rosa Granite, Western Alps: petrological Rb–Sr and stable isotope data. *Contr. Miner. Petrol.* **55**, 147–179.

Giannini, E. & Lazzarotto, A. 1975. Tectonic evolution of the Northern Apennines. In: *Geology of Italy* (edited by Squyres, G.). The Earth Sciences Society of the Libyan Arab Republic, Tripoli, 237–287.

Giglia, G. 1967. Geologia dell' alta Versilia settentrionale. (Tav. M. Altissimo). *Mem. Soc. Geol. It.* **6**, 67–95.

Giglia, G. & Radicati di Brozolo, R. 1970. K/Ar age of metamorphism in the Apuane Alps (northern Tuscany). *Boll. Soc. Geol. It.* **89**, 485–497.

Guidotti, C. & Sassi, F. 1976. Muscovite as a petrogenetic indicator in pelitic schists. *N. Jb. Mineral. Abh.* **127**, 97–142.

Harrison, T. M. 1981. Diffusion of ^{40}Ar in hornblende. *Contr. Miner. Petrol.* **78**, 324–331.

Hunziker, J. C. 1974. Rb–Sr and K–Ar age determinations and the Alpine tectonic history of the Western Alps. *Mem. Ist. Geol. Mineral. Univ. Padova* **31**, 1–55.

Hurzeler, J. & Engesser, B. 1976. Les faunes de mammiferes neogenese du Bassin de Baccinello (Grossetto, Italie). *C. r. hebd. Seanc. Acad. Sci. Paris* **D283**, 333–336.

Kligfield, R. 1978. Continental margin deformation in the Northern Apennines, Italy: a structural study in the Alpi Apuane region. Unpublished Ph.D. thesis, Columbia University, New York.

Kligfield, R. 1979. The Northern Apennines as a collisional orogen. *Am. J. Sci.* **279**, 676–691.

Kligfield, R. 1980. Structural–geochronological constraints on plate tectonic models for the Corsica–Northern Apennine collision. In: *Evolution and tectonics of the Western Mediterranean and surrounding areas* (edited by Udias, A. and Channell, J. E. T.). Instituto Geografico Nacional, Spec. Publ. 201, Madrid, Spain, 163–178.

Kligfield, R., Carmignani, L. & Owens, W. H. 1981. Strain analysis of a Northern Apennines shear zone using deformed marble breccias. *J. Struct. Geol.* **3**, 421–436.

Kroner, A. & Clauer, N. 1979. Isotopic dating of low-grade metamorphic shales in northern Namibia (Southwest Africa) and implications for the orogenic evolution of the Pan-African Damara belt. *Precambrian Res.* **10**, 59–72.

Kübler, B. 1967. La cristallinite de l'illite et les zones tout a fait superieures du metamorphisme, *Etages tectoniques*, Colloque a Neuchatel. Editions de la Baconniere, Neuchatel, 105–122.

Lorenz, H. G. 1968. Stratigraphische und mikropalaontologische Untersuchungen des Braunkohlengebietes von Baccinello (Provinz Grossetto—Italien). *Riv. Ital. Paleont.* **74**, 147–270.

Odin, G. S., Hunziker, J. C. & Lorenz, C. R. 1975. L'age radiometrique du Miocene inferieur en Europe Occidentale et Centrale. *Geol. Rdsch.* **64**, 570–592.

Pffifner, O. A. & Ramsay, J. G. 1982. Constraints on geological strain rates: arguments from finite strain states of naturally deformed rocks. *J. Geophys. Res.* **87**, 311–321.

Purdy, J. W. & Jäger, E. 1976. K–Ar Ages on rock-forming minerals from the central Alps. *Mem. Ist. Geol. Mineral. Univ. Padova* **30**, 1–32.

Rau, A. & Tongiorgi, M. 1974. Geologia dei Monti Pisani a Sud-Est della valle del Guappero. *Mem. Soc. Geol. It.* **13**, 227–408.

Steiger, R. H. & Jäger, E. 1977. Subcommission on geochronology: convention on the use of decay constants in geo- and cosmochronology. *Earth Planet. Science Lett.* **37**, 359–362.

Spry, A. 1969. *Metamorphic Textures*. Pergamon Press, New York.

Tisserant, D. & Odin, G. 1979. Datation isotopique de glauconies miocenes d'Afrique du Nord-Ouest. *C. r. somm. Soc. geol. Fr.* **4**, 188–190.

Turner, G. 1970. Thermal histories of meteorites by the $^{39}Ar/^{40}Ar$ method. In: *Meteorite Research* (edited by Millman, P.). D. Reidel Publishing Company, Dordrecht, Holland, 407–417.

Vai, G. B. 1970. Evidence of Silurian in the Apuane Alps (Tuscany, Italy). *Giorn. Geol.* **38**, 349–372.

Velde, B. 1967. Si^{4+} Content of natural phengites. *Contr. Miner. Petrol.* **14**, 250–258.

Weber, K. 1972. Notes on determination of illite crystallinity. *N. Jb. Miner. Mh.* **6**, 267–276.